Robustness of delocalization to the inclusion of soft constraints in long-range random models

P. A. Nosov[1,2,3,*] and I. M. Khaymovich[3,†]

[1]*Department of Physics, St. Petersburg State University, St. Petersburg 198504, Russia*

[2]*NRC Kurchatov Institute, Petersburg Nuclear Physics Institute, Gatchina 188300, Russia*

[3]*Max-Planck-Institut für Physik komplexer Systeme, Nöthnitzer Straße 38, 01187-Dresden, Germany*

(Received 3 May 2019; published 28 June 2019)

Motivated by the constrained many-body dynamics, the stability of the localization-delocalization properties to the inclusion of soft constraints is addressed in random matrix models. These constraints are modeled by correlations in long-ranged hopping with the Pearson correlation coefficient different from zero or unity. Counterintuitive robustness of delocalized phases, both ergodic and (multi)fractal, in these models, is numerically observed and confirmed by the analytical calculations. First, the matrix inversion trick is used to uncover the origin of such robustness. Next, to characterize delocalized phases, a method of eigenstate calculation, sensitive to correlations in long-ranged hopping terms, is developed for random matrix models and approved by numerical calculations and the previous analytical ansatz. The effect of the robustness of states in the bulk of the spectrum to the inclusion of soft constraints is generally discussed for single-particle and many-body systems.

DOI: 10.1103/PhysRevB.99.224208

I. INTRODUCTION

Absence of thermalization in interacting many-body quantum systems has attracted significant interest and boosted numerous studies of different possibilities to violate the eigenstate thermalization hypothesis (ETH) both in static and driven systems. The first and most developed way to do this is to randomize system parameters by including disorder. This phenomenon is called many-body localization (MBL) [1,2]. Like in a single-particle case of Anderson localization [3], disorder induces destructive interference and provokes emergent local integrals of motion [4,5] blocking the excitation transport.

An alternative way to break ETH in absence of disorder is to add some hard constraints to the many-body system, that crucially reduce the Hilbert space by separating the Hamiltonian into the disjoint subblock structure, see Fig. 1(a). These hard constraints can be realized either by infinitely strong interactions [6–9], additional integrals of motion [10–12], or gauge invariance [13]. As a result, such hard constraints produce special low-entanglement states (such as many-body scars) in the bulk of the spectrum [6,7], giving significant contribution to the typical infinite-temperature states and revealing themselves via infinitely long-lived oscillations in quenched observables [14]. However, in real life, none of barriers is infinite. The effect of *soft* constraints on the thermalization in such systems is nontrivial and under hot debate nowadays as the finite-energy barriers between disjoint Hilbert space subblocks might be prevailed at high temperature, Figs. 1(c) and 1(e).

For this reason, it is of fundamental importance to study a simple model in which hard and soft constraints can be

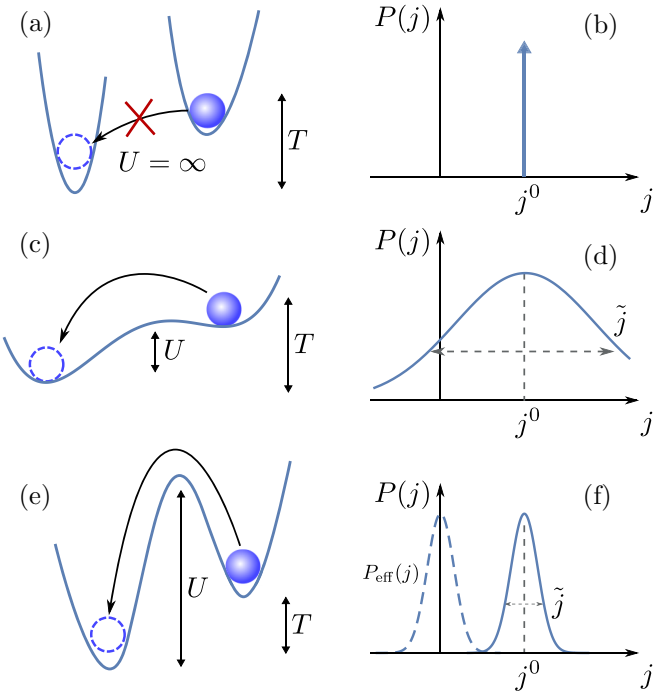

FIG. 1. Sketch of constraints in [(a), (c), and (e)] many-body systems and [(b), (d), and (f)] random matrix models. Hard constraint corresponds to (a) the infinite barrier $U=\infty$ between blocks of Hamiltonian (shown pictorially as parabolic potentials) at any temperature T and (b) the absence of any fluctuations $j^0/\tilde{j}=\infty$ in long-ranged hopping in random matrix analogs. The opposite limit of very small constraint allows large fluctuations in both cases [(c) and (d)] due to small ratios $U/T \ll 1$ and $j^0/\tilde{j} \ll 1$. The most nontrivial case of soft constraint with finite but large barrier $U/T \gg 1$ and $j^0/\tilde{j} \gg 1$ (e) provides the way to overcome the barrier with a thermal-activated rate in the many-body case and (f) suggests that delocalization is determined by the width of the distribution ($P_{\rm eff}$), but not by its peak position (P).

*p.nosov1995@gmail.com

†ivan.khaymovich@pks.mpg.de

easily realized and corresponding localization properties can be precisely investigated. This would provide efficient criteria to characterize the effects of soft constraints in generic cases.

The straightforward analog of hard constraints in single-particle systems is given, e.g., by fully correlated long-ranged hopping in random matrix models [15–19]. Indeed, in these models, the complete correlations of *all* hopping terms, Fig. 1(b), impose the hard constraints like in the case of many-body scars and localize the states in the bulk of the spectrum. However, due to the single-particle nature of these systems, all states in the spectral bulk become localized [20]. Soft constraints in this case can be easily realized by considering partial correlations of long-ranged hopping with noninteger Pearson correlation coefficient. In this work, we consider such single-particle disordered models with partially correlated long-ranged hopping, Figs. 1(d) and 1(f), investigate both numerically and analytically their eigenstate statistics and phase diagrams, and reveal unexpected robustness of delocalized phases to soft constraints, Fig. 1(f).

In most random matrices, the delocalized side of the localization transition (corresponding to ETH in many-body systems) is represented by Gaussian Wigner-Dyson ensembles [21]. One of most well-known examples of a d-dimensional random matrix model confirming this statement and demonstrating the Anderson localization transition (ALT) at any d (including $d \leqslant 2$) is the power-law random banded matrix ensemble (PLRBM) [22],

$$\hat{H} = \hat{\varepsilon} + \hat{j}, \quad \hat{\varepsilon} = \sum_n \varepsilon_n |n\rangle\langle n|, \tag{1a}$$

$$\hat{j} = \sum_{m,n} j_{mn} |m\rangle\langle n| \,, \tag{1b}$$

written in d-dimensional basis of N lattice sites $|n\rangle$. This model is characterized by the independent Gaussian distributed hopping terms j_{mn}, with the standard deviation $\langle j_{mn}^2\rangle^{1/2} \propto |m-n|^{-a}$ power-law decaying at large distances $|m-n| \gg 1$ and its ALT is governed by the decay exponent a responsible for the ratio of the on-site disorder $\varepsilon_n = H_{nn}$ [23] and hopping terms. The system shows ergodic (localized) wave-function statistics for $a < d$ ($a > d$), while the ALT point $a = d$ is characterized by so-called nonergodic extended (multifractal) wave functions typical for the ALT phase diagram at the criticality [24,25].

However recently there have been found several models showing the whole nonergodic extended phases, see, e.g., Refs. [19,26]. The milestone random matrix example in this row is the Rosenzweig-Porter ensemble (RP) [27]. This nominally 1d model has infinitely long-ranged independent Gaussian distributed hopping elements with the N-dependent variance $\langle j_{mn}^2\rangle \propto N^{-\gamma}$ and apart from the ALT transition at $\gamma = 2$ [28–34], it exhibits an ergodic transition (ET) at $\gamma = 1$ from the ergodic phase ($\gamma < 1$) to a whole phase of nonergodic extended states ($1 < \gamma < 2$) characterized by a nontrivial fractal support set [35,36] of wave functions [26] with the fractal Hausdorff dimension $D = 2 - \gamma$, $0 < D < 1$. This behavior has been further confirmed by several analytical and numerical papers [37–45].

The question of constraints (hopping correlations) imposed in both above mentioned models has been considered recently in Ref. [19]. Indeed, the new paradigm of the ALT suggested there states that hopping correlations $\langle j_{mn} j_{m'n'}\rangle - \langle j_{mn}\rangle\langle j_{m'n'}\rangle \neq 0$ shrink in general an ergodic phase towards smaller disorder strengths extending both localized and multifractal phases. In the case when all hopping integrals are fully correlated (with unit Pearson's coefficient), the localization at any disorder strength is restored [15,18,46] similar to the case of the short-range Anderson model in $d = 1, 2$ [3,47]. An example of such random matrix models with fully correlated hopping elements $j_{m\neq n} = C|m-n|^{-a}$, decaying with the distance $|m-n|$ as a power-law like in PLRBM, has been suggested in a seminal paper by Burin and Maksimov (BM) [15]. The infinitely long-ranged limit of this model (analogous to RP) with complete correlations between hopping terms $j_{mn} = CN^{-\gamma/2}$ has been shown to be exactly integrable by Yuzbashyan and Shastry (YS) [16,17]. Both these models demonstrate localization for all eigenstates, except measure zero, for all values of parameters a and γ. Note that the statistics of the site-independent scalar $C \sim 1$ does not play any role here.

A representative type of correlations considered in Ref. [19] is the hard constraint (correlations with Pearson's coefficient $+1$) of *certain* pairs, (m, n) and (m', n'), of hopping terms,

$$j_{mn}/j_{m'n'} = f(m,n)/f(m',n') > 0 \,. \tag{2}$$

Here, $f(m, n) > 0$ is the deterministic function of indices m, n, and possibly of the system size N. For uncorrelated models (like PLRBM and RP) the pairs are only $(m', n') = (n, m)$, while in fully correlated examples (BM and YS) all pairs of (m', n') and (m, n) are involved. In the intermediate translation-invariant case, $|m' - n'| = |m - n|$ [20].

In this paper, we address a complimentary aspect of soft constraints, namely, *partial* hopping correlations of *all* pairs of hopping terms

$$0 < \langle j_{mn} j_{m'n'}\rangle < \sqrt{\langle j_{mn}^2\rangle\langle j_{m'n'}^2\rangle} \,. \tag{3}$$

For this we consider both PLRBM and RP models with *finite* hopping average values that interpolate between original uncorrelated PLRBM and RP ensembles and their fully correlated counterparts, BM and YS models [48]. The unexpected stability of the delocalized phases to soft constraints in both cases is demonstrated. The delocalization is shown to survive even for relatively narrow distributions with mean values j^0 much larger than the width $\tilde{j}$, see Fig. 1(f). The positions of the ALT and possible ET are shown to be governed solely by the distribution width $\tilde{j}$, but not by relative fluctuations $\tilde{j}/j^0$, see Fig. 2 and P_{eff} in Fig. 1(f). This brings us to the conclusion that soft constraints added to the initially delocalized phase do not break delocalization of any state in the bulk of the spectrum, Fig. 1(e), even if the hard constraint does, Fig. 1(a).

In order to uncover the origin of this counterintuitive result, we first use the matrix inversion trick suggested in Ref. [19] to rewrite the eigenproblem in the coordinate basis in an alternative way. Furthermore we develop the self-consistent method of eigenvector calculation based on the averaging over off-diagonal matrix elements, allowing one to access wave-function statistics and, in particular, confirming the phenomenological ansatz known in the literature for RP

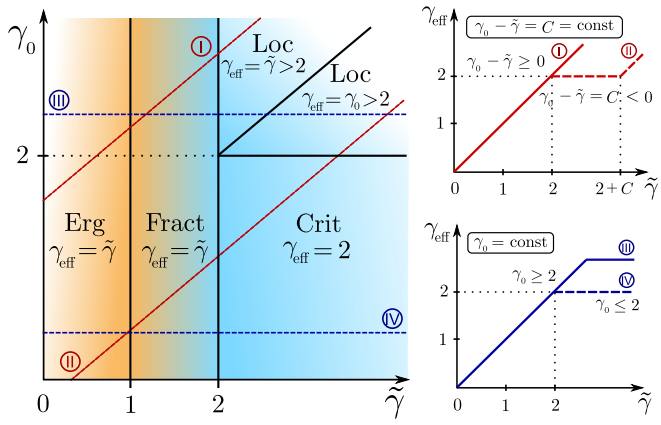

FIG. 2. Phase diagram of RP model with partial correlations (5) with average hopping $j^0 \sim N^{-\gamma_0/2}$ and its standard deviation $\tilde{j} \sim N^{-\tilde{\gamma}/2}$. (left) Both the Anderson localization transition, $\gamma_{\rm eff} = 2$, and the ergodic transition, $\gamma_{\rm eff} = 1$, are governed solely by $\tilde{\gamma}$, while $\gamma_{\rm YS} = \max(\gamma_0, 2)$ (12) affects wave-function profile only in the localized phase at $\gamma_{\rm YS} < \tilde{\gamma}$. Right panels show the behavior of $\gamma_{\rm eff}$ along different cuts (I-IV) shown in left panel.

ensemble [42–44] (see also Ref. [38]). Unlike the standard renormalization group analysis [22,49] or the Wigner-Weisskopf approximation [42] used in the literature before, this self-consistent method is sensitive to the hopping correlations. In the current problem, the full ALT diagram of previously mentioned models is calculated with help of these methods.

The rest of the paper is organized as follows. In Sec. II, we formulate the random matrix models in the focus. Section III shows how the naive guess for the behavior of these models fails, and provide numerical results along with localization-delocalization phase diagrams. Section IV describes the matrix inversion trick which explains the behavior of these models and allows us to uncover the origin of unexpected stability of delocalized phases. In Sec. V, we demonstrate the self-consistent method of eigenfunction calculation on the example of RP ensemble with finite mean hopping values. In Conclusion, we sum up our results and give an outlook.

II. MODELS

Throughout the text we focus on the generalized Anderson's single-particle model with long-ranged hopping terms, represented by the Hamiltonian (1). The uncorrelated diagonal disorder is given by independent identically distributed random on-site energies ε_n with zero mean and fixed variance

$$\langle \varepsilon_n \rangle = 0 \,, \quad \langle \varepsilon_n^2 \rangle = W^2 . \tag{4}$$

The summation in (1b) is taken over pairs of sites m, n coupled by hopping integrals

$$j_{mn} = j_{nm}^* = j^0(|m-n|) + h_{mn}\tilde{j}(|m-n|) \,, \tag{5}$$

characterized by the distant-dependent mean and standard deviation values, respectively,

$$\langle j_{mn} \rangle = j^0(|m-n|) \,, \quad \sigma_j = \tilde{j}(|m-n|) \,, \tag{6}$$

where $\sigma_j^2 = \langle j_{mn}^2 \rangle - \langle j_{mn} \rangle^2$. For simplicity, we restrict our consideration to $d = 1$, unless stated otherwise. Here and further, we denote by h_{mn} i. i. d. random variables with zero mean $\langle h_{mn} \rangle = 0$ and unit variance $\langle |h_{mn}|^2 \rangle = 1$.

The PLRBM and RP ensembles correspond to $j^0 = 0$ and

$$\tilde{j}_{\rm PLRBM} = \frac{1}{|m-n|^{\tilde{a}}} \quad \text{and} \quad \tilde{j}_{RP} = N^{-\tilde{\gamma}/2} \,, \tag{7}$$

respectively, while for BM and YS models in contrast $\tilde{j} = 0$,

$$j^0_{\rm BM} = \frac{1}{|m-n|^{a_0}} \,, \quad \text{and} \quad j^0_{\rm YS} = N^{-\gamma_0/2} \,. \tag{8}$$

As infinitely long-ranged models (like RP and YS) do not have the notion of distance, the main tool used to characterize the properties of their delocalized and localized phases is the standard multifractal (MF) analysis. This analysis is based on the spectrum of fractal dimensions [50]

$$f(\alpha) = 1 - \alpha + \lim_{N\to\infty} \ln[P(|\psi_E(n)|^2 = N^{-\alpha})]/\ln N \,, \tag{9}$$

defined via the distribution of wave-function amplitudes $P(|\psi_E(n)|^2)$ with the N scaling of eigenfunctions $|\psi_E(n)|^2 \propto N^{-\alpha}$, see Fig. 3.

Other long-ranged models (like PLRBM and BM) provide additional tools, e.g., the spatial decay of eigenfunctions with the distance $|n - n_0|$ from its maximal value at $n = n_0$ [18,19] given by the typical wave-function decay, see Fig. 4,

$$|\psi_E(n)|^2_{\rm typ} \equiv \exp[\langle \ln |\psi_E(n)|^2 \rangle] \sim |n - n_0|^{-a_{\rm eff}} \,. \tag{10}$$

Here $\langle \ldots \rangle$ denotes the average over disorder and over eigenstates in the middle of the spectrum. The energy level statistics (see, e.g., Ref. [51]) as basis-invariant characteristics gives the definite information about the fully ergodic (Wigner-Dyson) phase and the phase localized in a certain basis with the Poisson level statistics [19,52].

For RP model, the spectrum of fractal dimensions $f(\alpha)$ is shown to be linear in $\alpha = -\ln|\psi_E(n)|^2/\ln N$ for $\tilde{\gamma} \geqslant 1$, with the slope 1/2 [26]

$$f(\alpha) = \begin{cases} 1 + (\alpha - \tilde{\gamma})/2, & \alpha_{\rm min} < \alpha < \tilde{\gamma} \\ -\infty, & \alpha < \alpha_{\rm min} \text{ or } \alpha > \tilde{\gamma} \end{cases} , \tag{11}$$

and an additional point $f(0) = 0$ for $\tilde{\gamma} > 2$. Here, $\alpha_{\rm min} = \max(0,\ 2 - \tilde{\gamma})$. The $f(\alpha)$ in the ergodic phase, $\tilde{\gamma} < 1$, coincides with the one at $\tilde{\gamma} = 1$ and is represented by the only point $f(1) = 1$ [26].

The Yuzbashyan-Shastry (YS) ensemble (or as sometimes called the Type-I model) [16–18,46,53] characterized by deterministic infinitely long-range hopping terms $j_{mn} = j^0 g_m g_n$, with the constants $g_m \propto O(1)$ of order of one, is exactly integrable [16,17] and known to have all localized states for $j^0 < 1/N$ and all, except one, localized states for $j^0 > 1/N$ [17,19,46,53]. The generalization of this ensemble to N-dependent hopping elements (8) shows a single-site localized phase for $\gamma_0 > 2$ and a critical behavior at $\gamma_0 < 2$ with the spectrum of fractal dimensions given by (11) with γ_0 replaced by the following expression [19] (see Appendix A for analytical derivations)

$$\gamma_{\rm YS} = \max(\gamma_0,\ 2) \geqslant 2 \,. \tag{12}$$

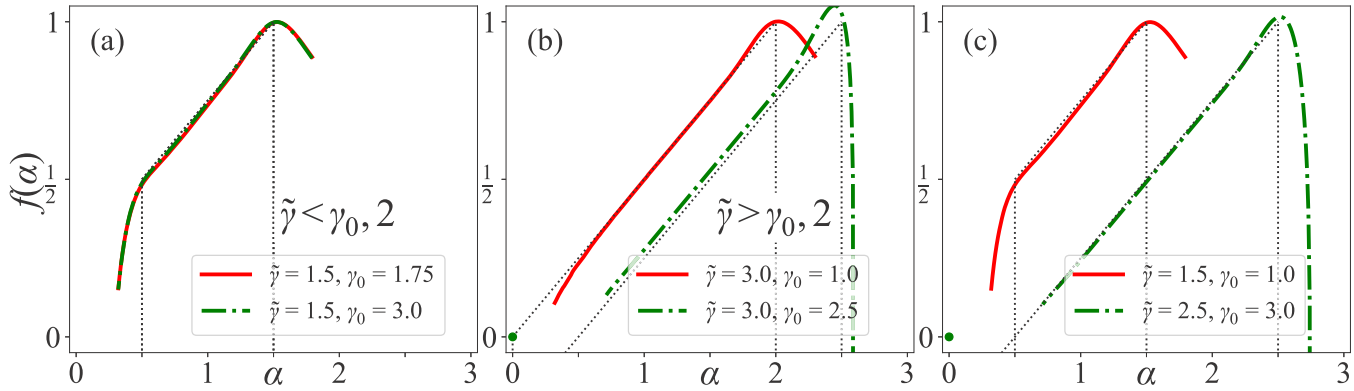

FIG. 3. Spectrum of fractal dimensions $f(\alpha)$ of RP model with partial correlations (5) for different scaling of the average hopping $j^0 \sim N^{-\gamma_0/2}$ and its standard deviation $\tilde{j} \sim N^{-\tilde{\gamma}/2}$. The finite-size data are numerically extrapolated to infinity from system sizes $N = 2^9 \dots 2^{14}$ with $N_r = 10^3$ disorder realizations in each. Dashed lines show analytical predictions (11) and (17a) for $f(\alpha)$. (a) The naively expected case of small $\tilde{\gamma} < \gamma_0, 2$ with fluctuations $\tilde{j} \gg j^0$ dominating over correlated hopping j^0 and determining the corresponding delocalized phase by $\gamma_{\text{eff}} = \tilde{\gamma}$. (b) The case of large $\tilde{\gamma} > \gamma_0, 2$ where correlated hopping dominates $j^0 \gg \tilde{j}$ and localized the system with $\gamma_{\text{eff}} = \gamma_{\text{YS}} = \max(\gamma_0, 2) \geqslant 2$. (c) Nontrivial case $\min(\gamma_0, 2) < \tilde{\gamma} < \max(\gamma_0, 2)$ showing the dominant correlated hopping $j^0 \gg \tilde{j}$, with the phase governed solely by $\gamma_{\text{eff}} = \tilde{\gamma}$.

PLRBM undergoes the ALT at $a = 1$, showing ergodic behavior at $a < 1$ and power-law localization at $a > 1$ [24,25], with the decay rate equal to the parameter a

$$|\psi_E(n)| \propto |\psi_E(n_0)|/|n - n_0|^a \tag{13}$$

at the large distance $|n - n_0| \gg 1$ from the maximal point n_0, $\max_n |\psi_E(n)| = |\psi_E(n_0)|$.

In BM model [15,18,19,46,54–57], the fully correlated counterpart of PLRBM, which is determined by the Hamiltonian (1) with the hopping elements (8), all, except measure zero of the states, are power-law localized (13) in the entire region of the parameter a. However, the power-law decay rate a_{BM} is not equal to a, but instead is always larger than one (see Refs. [18,19] for details)

$$a_{\text{BM}} = \max(a,\ 2 - a) \geqslant 1\ . \tag{14}$$

III. INTUITIVE GUESS AND NUMERICAL RESULTS

What would be the phase diagram for general models (1–6) with both finite mean j^0 and fluctuating $\tilde{j}$ hopping terms? For the first glance, it is natural to expect that the behavior of uncorrelated models (7) should be dominant as soon as $\tilde{j} \gg j^0$ ($\tilde{\gamma} < \gamma_0$ or $\tilde{a} < a_0$) as the distribution of hopping elements is relatively wide and nearly centered at zero, see Fig. 1(d), and vice versa the models with deterministic hopping (8) should dominate at $\tilde{j} \ll j^0$ ($\tilde{\gamma} > \gamma_0$ or $\tilde{a} > a_0$) when the distribution is relatively narrow and its width can be neglected, Figs. 1(b) and 1(f).

However, this is not the case. Indeed, from the numerical calculations, one can see that these models undergo the ALT (and the ET for RP case) at the same points as their uncorrelated counterparts: $\tilde{\gamma} = 2$ ($\tilde{\gamma} = 1$) and $\tilde{a} = 1$ irrespective to the amplitude j^0 as if all mean values are zero, $j^0 = 0$, Fig. 2. Moreover, the wave-function statistics of such models in all

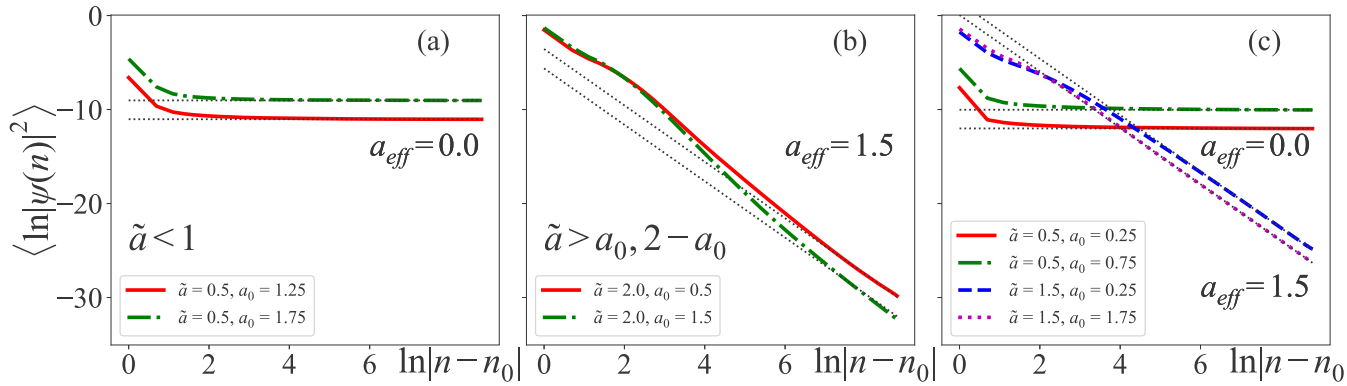

FIG. 4. Typical wave-function spatial decay $\ln|\psi_E(n)|^2_{\text{typ}} = \langle \ln(|\psi_E(n)|^2) \rangle$ vs n for PLRBM model with partial correlations (5) for different power-law decay rates of the average hopping $j^0_n \sim |n|^{-a_0}$ and its standard deviation $\tilde{j}_n \sim |n|^{-\tilde{a}}$. The data are numerically calculated for the system size $N = 2^{14}$ and $N_r = 10^3$ disorder realizations. Dashed lines show analytical predictions (13, 17b) of this power-law decay. Panels show the cases similar to ones in Fig. 3: (a) small $\tilde{a} < 1, a_0$ with dominant fluctuations $\tilde{j} \gg j^0$ leading to the expected ergodic phase and $a_{\text{eff}} = \tilde{a}$; (b) large $\tilde{a} > a_0, 2 - a_0$ where correlated hopping dominates $j^0 \gg \tilde{j}$ and the localized phase is governed by $a_{\text{eff}} = a_{\text{BM}} = \max(a_0, 2 - a_0)$; (c) nontrivial case $\min(a_0, 2 - a_0) < \tilde{a} < \max(a_0, 2 - a_0)$ of dominant correlated hopping $j^0 \gg \tilde{j}$ governed solely by $a_{\text{eff}} = \tilde{a}$. The data with $\tilde{a} < 1$ in panels (a) and (c) are shifted with respect to each other for clarity.

phases, Figs. 3 and 4, coincides with the one of a simple mixture of two uncorrelated long-ranged hopping models of the type (7), with hopping terms

$$j_{mn} = h_{mn}\tilde{j}(|m-n|) + h^0_{mn}\tilde{j}^0(|m-n|)\,, \tag{15}$$

where the function $\tilde{j}^0(|m-n|)$ is described by (8) with the parameters γ_0 and a_0 of fully correlated models (YS and BM) replaced by their effective values (12) and (14), respectively. Thus, in the leading approximation, one can replace the mixture of hopping elements by their maximum

$$j_{mn} = h_{mn}\max[\tilde{j}(|m-n|), \tilde{j}^0(|m-n|)] \tag{16}$$

and map the model with partial correlations to the one with zero mean (equivalent to RP and PLRBM) and parameters γ and a in Eqs. (11) and (13) replaced by effective ones

$$\gamma_{\rm eff} = \min(\tilde{\gamma}, \gamma_{\rm YS}) = \min(\tilde{\gamma}, \max(\gamma_0, 2))\,, \tag{17a}$$

$$a_{\rm eff} = \min(\tilde{a}, a_{\rm BM}) = \min(\tilde{a}, \max(a_0, 2-a_0))\,. \tag{17b}$$

This is the main result of this paper shown here numerically, Figs. 3 and 4, and confirmed further analytically.

The qualitative explanation of this unexpected stability of delocalized states originates from the fact that the models with deterministic long-range hopping terms (like YS and BM) demonstrate only localized eigenfunction statistics in the bulk of the spectrum, but never delocalized. As a result, in the mixture these fully correlated models can compete with their uncorrelated counterparts only in the localized phase, $\tilde{a} > 1$ or $\tilde{\gamma} > 2$, Fig. 2, affecting the wave-function spatial profile in the locator expansion [3,49,58] (see also Ref. [19] for more detailed discussion). In terms of soft constraints, this means that, as soon as typical states in the spectral bulk are considered, the infinite temperature corresponding to them prevail over the finite barrier of soft constraint between previously disjoint subblocks of the Hamiltonian and brings the system to the phase where it was before imposing constraints.

To understand the origin of the above mentioned behavior of partially correlated models (3), summarized in Eqs. (15)–(17a), in the next section, we describe a matrix inversion trick [19] providing an alternative representation of the eigenproblem and apply it to the mixture of YS and RP model as an example.

IV. MATRIX INVERSION TRICK

Here we restrict our consideration of the matrix inversion trick to the case of the mixture of RP and YS models (for the mixture of PLRBM and BM models please see Appendix B). For the first time, this method has been suggested by us in Ref. [19] to analytically prove the duality of the eigenfunction power-law decay in the 1d BM model (14) numerically discovered in Ref. [18] and to generalize both Anderson localization [3,49,58] and Mott ergodicity [59] principles for the models with correlated hopping. However recently there have been found several many-body [60,61] and higher-dimensional, $d > 1$, single-particle models [62,63], applied to which this method easily uncovers their phase diagrams and the wave-function structure by the extension the locator expansion validity range.

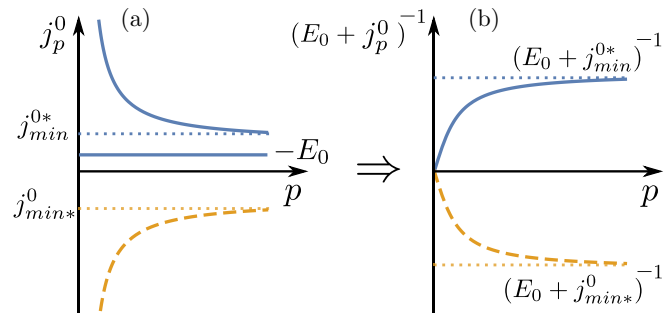

FIG. 5. Sketch of the spectrum of deterministic hopping (18), (a) diverging from either (solid blue line) or both (blue and yellow lines) sides, but has a finite gap, and (b) spectrum of the inverse matrix $\hat{M}$ (19) with diminished divergence(s).

Let's first consider the pure deterministic (BM or YS) model (8). The matrix inversion trick is based on the spectral properties of the hopping matrix

$$\hat{j}^0 = \sum_{\langle m,n\rangle} j^0(|m-n|)|m\rangle\langle n| \equiv \sum_p j^0_p|p\rangle\langle p| \tag{18}$$

diagonalized in a certain basis $|p\rangle$ (momentum basis for BM model). If the spectrum j^0_p of this matrix diverges from either side in the thermodynamic limit (e.g., $j^0_{\rm max} = \max_p j^0_p \to \infty$ for $N \to \infty$ and $j^0_{\rm min} = \min_p j^0_p$ is finite) or even from both sides, but has a finite spectral gap, see Fig. 5(a), one can diminish the effect of these divergent terms to the hopping elements, inverting the matrix $(1 + \hat{j}^0/E_0) \equiv \hat{M}^{-1}$

$$\hat{M} = (1 + \hat{j}^0/E_0)^{-1} = \sum_p \frac{|p\rangle\langle p|}{1 + j^0_p/E_0}\,. \tag{19}$$

This matrix inversion sends the diverging top-spectrum (or edge-spectrum) terms close to $j^0_{\rm max}$ to the denominator of the sum while the condition $E_0 + j^0_{\rm min} > 0$ avoids the divergence of the contributions from the bottom (or states close to the gap) of the spectrum, see Fig. 5(b). The optimization of $E_0 \sim N^\beta$ over the parameter β [19] gives the smallest effective hopping terms at $\beta = 0$ in the whole parameter range (please see Appendix B for details).

After the matrix inversion trick the problem takes the form

$$[(1 + \hat{j}^0/E_0)^{-1}(E - \hat{\varepsilon} + E_0) - E_0]|\psi_E\rangle = 0\,. \tag{20}$$

The diagonal part M_0 of the matrix $(1 + \hat{j}^0/E_0)^{-1}_{m,n} = M_{m-n}$ forms effective on-site disorder $M_0\varepsilon_n$ and eigenvalue $M_0(E + E_0) - E_0$ of the problem, while the hopping terms are formed by $M_{m-n\neq 0}(E - \varepsilon_n + E_0)$.

The main idea behind this matrix inversion trick uses the fact that the eigenstates with large hopping energies $|j^0_p| \gg 1$ are barely affected by the disorder $\hat{\varepsilon}$. Thus they nearly coincide with those hopping matrix eigenstates $|p\rangle$ that give the main contribution to (18). All other eigenstates corresponding to small hopping energies $|j^0_p| \sim O(1)$ are orthogonal to these large-energy states at the spectral edge and thus almost orthogonal to the main contribution to the hopping matrix given by them. As a result the states in the bulk of the spectrum "see" the hopping terms $M_{m-n\neq 0}(E - \varepsilon_n + E_0)$ which are significantly reduced compared to the initial ones j^0_{m-n}.

For the case of YS model the rank-1 matrix $\hat{j}^0$ has the only nonzero eigenvalue $j^0_{p=0} = N^{1-\gamma_0/2}$ corresponding to the zero-momentum state $\langle n|0\rangle_p = N^{-1/2}$ with arbitrary rest basis states $|g_{k\neq 0}\rangle$ orthonormal to $|0\rangle_p$ [64].

The same matrix inversion trick (20) can be applied as well to the model (6) with partial correlations (3)

$$[(1+\hat{j}^0/E_0)^{-1}(E-\hat{\varepsilon}-\hat{\tilde{j}}+E_0)-E_0]|\psi_E\rangle = 0\,, \tag{21}$$

where we inverse only the deterministic hopping part with the semi-infinite spectrum.

As a result Eq. (21) takes the predicted form of Eq. (15)

$$[\hat{\varepsilon}+\hat{\tilde{j}}+\hat{\tilde{j}}^0+\hat{r}]|\psi_E\rangle = E|\psi_E\rangle\,. \tag{22}$$

with the fluctuating elements of the matrix $\hat{\tilde{j}}^0$

$$\tilde{j}^0_{mn} = -\frac{E-\varepsilon_n+E_0}{N+E_0N^{\gamma_0/2}} \sim N^{-\gamma_{\rm YS}/2}\,, \tag{23}$$

which do not break the locator expansion and the residual term $\hat{r}$ small compared to $\hat{\tilde{j}}$

$$r_{mn} = \frac{\sum_l \tilde{j}_{\rm ln}}{N+E_0N^{\gamma_0/2}} \sim \frac{N^{(1-\tilde{\gamma})/2}}{N+E_0N^{\gamma_0/2}} \ll \tilde{j}_{mn}\,. \tag{24}$$

In Eq. (23), $\gamma_{\rm YS}$ is given by (12). This derivation confirms our numerical observation (15) and concludes this section. The consideration of the mixture of PLRBM and BM models is addressed in Appendix B.

To sum up, in this section, we have shown that the effective locator expansion result [19] analogous to (13) is applicable in the case of the RP-YS mixture to calculate the wave function in the whole localized phase coinciding with the one of the uncorrelated model ($\tilde{\gamma} > 2$) at any γ_0, Fig. 2. To calculate the wave-function statistics in *all* phases, including delocalized ones, in the next section we develop a self-consistent method sensitive to hopping correlations.

V. SELF-CONSISTENT EIGENSTATE CALCULATION

In this section, we consider the self-consistent method of the wave-function calculation, generalizing the perturbation theory. For simplicity, we restrict our consideration to the mixture of RP and YS ensembles. For more general analysis, please see Appendix C. Separating hopping terms $j_{mn} = j^0 + h_{mn}\tilde{j}$ (5) in the Hamiltonian (1) into deterministic $j^0 = j^0_{YS} = N^{-\gamma_0/2}$ (8) and fluctuating $\tilde{j} = \tilde{j}_{RP} = N^{-\tilde{\gamma}/2}$ (7) parts in the eigenproblem

$$(E_n-\varepsilon_k)\psi_{E_n}(k) = j^0\sum_l \psi_{E_n}(l) + \tilde{j}\sum_l h_{kl}\psi_{E_n}(l)\,, \tag{25}$$

one can formally write its solution

$$\psi_{E_n}(k) = \psi_{E_n}(n)\frac{J_{kn}}{\varepsilon_n-\varepsilon_k+J_{nn}}\,, \tag{26a}$$

$$J_{kn} \equiv a_n + P_{kn} + \tilde{j}h_{kn}\,. \tag{26b}$$

in terms of the sums

$$a_n = j^0\sum_l \psi_{E_n}(l)/\psi_{E_n}(n)\,, \tag{27a}$$

$$P_{kn} = \tilde{j}\sum_{l\neq n} h_{kl}\psi_{E_n}(l)/\psi_{E_n}(n) \tag{27b}$$

and $E_n - \varepsilon_n = J_{nn}$ given by (26b), that should be calculated self-consistently. Here and further we choose the index n in the energy E_n in such a way that in absence of off-diagonal elements $j^0 = \tilde{j} = 0$ the wave function is localized at $k = n$, $\psi_{E_n}(k) = \delta_{k,n}$, with the energy $E_n = \varepsilon_n$.

Averaging (26) over the hopping elements h_{mn} with fixed bare energies ε_n gives the following expression for the wave-function intensity

$$\left\langle\left|\psi_{E_n}(k)\right|^2\right\rangle_{h_{kn}} \sim \frac{\left\langle\left|\psi_{E_n}(n)J_{kn}\right|^2\right\rangle}{(\varepsilon_n-\varepsilon_k+\Delta E_n)^2+\Gamma_n^2}\,. \tag{28}$$

Here we assume that the sums P_{mn} and a_n are self-averaging and thus they are uncorrelated from each other and from h_{kl}. For RP model itself this approximation of self-averaging over hopping terms has been used in several papers [37,38] and confirmed there by other methods. The fluctuating energy shift $J_{nn} = E_n - \varepsilon_n$ after this averaging leads both to the energy shift ΔE_n and the level broadening Γ_n in Eq. (28). Both ΔE_n and Γ_n are of the same order as $E_n - \varepsilon_n$ and in principle contain contributions from all cumulants of P_{nn} and a_n, however for our analysis it is enough to consider only mean values and the first-order perturbation theory term $\tilde{j}h_{nn}$ with standard deviation $\tilde{j}$ taken into account (for further details see Appendix C)

$$\Gamma_n \simeq \langle a_n\rangle + \langle P_{nn}\rangle + \tilde{j}\,. \tag{29}$$

Here, Γ_n plays a role of the level broadening. This level broadening determines the size of the miniband of almost fully correlated eigenfunctions like in RP model [26,44]. The factor $\langle|\psi_{E_n}(n)J_{kn}|^2\rangle$ in the numerator of Eq. (28) guarantees the wave-function normalization and not important for the wave-function statistics.

Focusing on the N scaling of $\Gamma_n \sim \Delta E_n$ one can show that the localized state realizes at Γ_n smaller than the mean level spacing $\delta \simeq W/N$ of the model without hopping, the ergodic state corresponds to Γ_n large compared to the bare band of the system $W \sim O(1)$, while the fractal phase appears at intermediate values:

$$\begin{array}{ll} \Gamma_n \ll \delta & \Leftrightarrow \text{ localized phase} \\ \delta \ll \Gamma_n \ll N\delta \sim W & \Leftrightarrow \text{ fractal phase} \\ \Gamma_n \gg N\delta & \Leftrightarrow \text{ ergodic phase} \end{array}\,. \tag{30}$$

In order to estimate the scaling of the level broadening and identify, the corresponding phases one can make use of the self-consistent equations for P_{kn} and a_n which could be obtained by substituting expressions (26) for $\psi_{E_n}(k)$ and E_n to

(27). The resulting equations read as

$$a_n = j^0\left(1+\sum_{l\neq n}\frac{a_n+\tilde{j}h_{\ln}+P_{\ln}}{\varepsilon_n-\varepsilon_l+J_{nn}}\right), \tag{31a}$$

$$P_{kn} = \sum_{l\neq n}\frac{\tilde{j}h_{kl}(a_n+P_{\ln}+\tilde{j}h_{\ln})}{\varepsilon_n-\varepsilon_l+J_{nn}}. \tag{31b}$$

The next essential step is to average these equations over h_{nm} relying on the above-mentioned self-averaging properties of these sums. As a result, Eqs. (31) take the form

$$\langle P_{kn}\rangle = \tilde{j}^2 S_1\delta_{k,n}, \tag{32a}$$

$$\langle a_n\rangle = \frac{1}{(j^0)^{-1}-S_1} \sim \min\left(j^0, S_1^{-1}\right), \tag{32b}$$

with the sum S_1 given by

$$S_1 = \sum_l \frac{1}{\varepsilon_n-\varepsilon_l+\Gamma_n}. \tag{33}$$

The latter can be calculated, e.g., in two limiting cases of (i) the completely rigid spectrum $\varepsilon_n-\varepsilon_m=(n-m)\delta$, with δ being a bare mean level spacing without hopping, and (ii) the Poisson statistics of ε_n. Up to prefactors unimportant for the multifractal analysis S_1 takes the form

$$S_1(\Gamma_n) \sim \begin{cases} 1/\delta & \Gamma_n \ll N\delta \\ N/\Gamma_n & \Gamma_n \gtrsim N\delta \end{cases}. \tag{34}$$

Considering cases (30) and substituting (34) into (32) and (29) one easily obtains the result up to prefactors $O(1)$

$$\Gamma_n \sim \begin{cases} N^{-\min(\tilde{\gamma},\gamma_{\rm YS})/2} & \tilde{\gamma}>2, \text{ localized} \\ N^{1-\tilde{\gamma}} & 1<\tilde{\gamma}<2, \text{ fractal} \\ N^{(1-\tilde{\gamma})/2} & \tilde{\gamma}<1, \text{ ergodic} \end{cases}, \tag{35}$$

with $\gamma_{\rm YS}=\max(\gamma_0,2)$ given by (12).

Comparison of the resulting Γ_n with the one of the RP model shows the same N scaling with the parameter $\tilde{\gamma}$ replaced by $\gamma_{\rm eff}$ from Eq. (17a). One can also check it by the direct calculation of the multifractal spectrum. Indeed, the resulting approximate wave function (28) scales as

$$\left\langle\left|\psi_{E_n}(k)\right|^2\right\rangle_{h_{kn}} \sim \frac{N^{-\tilde{\gamma}}+N^{-\gamma_{\rm YS}}}{N^{-p}+\Gamma_n^2}, \tag{36}$$

where the scaling of $\Delta E_n\sim\Gamma_n$ is given by (35) and we parameterized $(\varepsilon_n-\varepsilon_k)\sim N^{-p/2}$ with the parameter p. For a certain distribution of the diagonal terms ε_n with the width $W\sim O(1)$ the scaling of the probability reads as

$$P(\varepsilon_n-\varepsilon_k)d\varepsilon_n = P(N^{-p/2})N^{-p/2}dp \sim N^{-p/2}dp \tag{37}$$

for positive $p>0$ as $P(\varepsilon_n\to 0)\sim O(1)$. For negative $p<0$ the probability is at least exponentially small in ε_n and thus, for multifractal analysis one should neglect it focusing on $p\geqslant 0$. As a result the spectrum of fractal dimensions

$$N^{f(\alpha)-1}d\alpha = P\left(\left|\psi_{E_n}\right|^2\sim N^{-\alpha}\right)d\left(\left|\psi_{E_n}(k)\right|^2\right) \tag{38}$$

can be found from the expression

$$N^{f(\alpha)-1}d\alpha = dP\left(N^{-\alpha}\sim\frac{N^{-\tilde{\gamma}}+N^{-\gamma_{\rm YS}}}{N^{-p}+\Gamma_n^2}\right) = \max_{p>0}N^{-p/2}d\alpha, \tag{39}$$

where the maximization in right-hand side is taken with respect to the condition $N^{-\alpha}\sim(N^{-\tilde{\gamma}}+N^{-\gamma_{\rm YS}})/(N^{-p}+\Gamma_n^2)$. The maximal probability is given by the condition $0<p<-2\ln\Gamma_n/\ln N$ leading to $p=\gamma_{\rm eff}-\alpha$ and to the result (11) with $\gamma_{\rm eff}$ given by (17a). Moreover the boundaries $0<p<-2\ln\Gamma_n/\ln N$ provide the correct bounds for α

$$\max(0,2-\gamma_{\rm eff})<\alpha<\gamma_{\rm eff}. \tag{40}$$

This analysis confirms numerical results shown in Fig. 3 and concludes this section. Note that the method developed in this section is powerful and accurate for the multifractal analysis as one can take into account cumulants of any order of the sums (31) fluctuating with the hopping terms and sensitively distinguish models with slightly different hopping correlations.

VI. CONCLUSION AND DISCUSSIONS

To sum up, in this work we address the effect of soft constraints on the phase diagram of random matrix models with long-ranged correlated hopping. We demonstrate unexpected robustness of the delocalized phases to partial hopping correlations imposed by soft constraints and determine wave-function statistics and corresponding phase diagrams of milestone disordered long-range models, power-law banded random matrix and Rosenzweig-Porter ensembles. This main result (17) is confirmed by both numerical calculations and two analytical approaches. The matrix-inversion trick developed in Ref. [19] uncovers the effective Hamiltonian (22) and confirms the wave-function behavior in the localized phase. The self-consistent method allows to calculate wave-function statistics in delocalized phases as well and confirm the main result of the paper.

A parallel drown between constrained random-matrix models and many-body systems, brings us to the conclusion that in general soft constraints added to the initially delocalized phase do not break delocalization of any typical (infinite temperature) state, even if the hard constraint does. Indeed, the infinite temperature corresponding to the typical states in the spectral bulk prevail over the finite barrier of soft constraint between previously disjoint subblocks of the Hamiltonian and brings the system to the phase where it was before imposing constraints. However, the relations of slow-dynamics phenomena [65] to hard and soft constraints both in many-body systems [6–13,66–69] and in closely related single-particle disordered models [44,70] is still under debates and consideration. The question of the dynamics and relaxation of highly nonlocal operators [71] is also in the focus of the research in the community.

Another intriguing question is how the interplay between partial correlations in hopping and interaction amplitudes could affect localization properties in many-body systems with either or both hopping and interaction terms being long-ranged in the coordinate space. Specifically, the limiting fully correlated case of the interacting version of Burin-Maksimov model was recently analyzed in Refs. [60,72–76], and the opposite situation without any constraints was considered in details in Refs. [77–82]. However, the intermediate regime represented by both finite means and dispersion in distribution functions of matrix elements needs deep consideration.

Finally, in order to more precisely investigate the role of partial correlations in long-range random matrix models, it would be insightful to construct the corresponding effective field-theoretic description with imposed soft constraints. For instance, this approach may naturally incorporate ergodicity-breaking phenomena in gauge-invariant lattice models [13]. Although the desirable theory is more technically involved than usual super-symmetric nonlinear sigma model due to finite means of hopping and effective nonlocality, several attempts were made to describe systems with correlations in off-diagonal terms [53,83]. Moreover, so-called "virial expansion" for almost diagonal random matrices developed in Refs. [84,85] seems to be a suitable candidate for an appropriate representation of constrained models with disjoint subblocks in Hilbert space.

ACKNOWLEDGMENTS

We are grateful to V. E. Kravtsov for stimulating discussions. P. N. appreciates warm hospitality of the Max-Planck Institute for the Physics of Complex Systems, Dresden, Germany, extended to him during his visits when this work was done. P.N. acknowledges funding by the RFBR, Grant No. 17-52-50013, and the Foundation for the Advancement to Theoretical Physics and Mathematics BASIS Grant No. 17-11-107. I.M.K. acknowledges the support of German Research Foundation (DFG) Grant No. KH 425/1-1 and the Russian Foundation for Basic Research Grant No. 17-52-12044.

APPENDIX A: YUZBASHYAN-SHASTRY MODEL

1. Model

Consider an ensemble of random $N \times N$ Hermitian matrices

$$H_0 = \operatorname{diag} \varepsilon + j^0 g^T g^* , \tag{A1}$$

with a random real vector $\varepsilon = (\varepsilon_1, \ldots, \varepsilon_N)$ and deterministic complex vector $g = (g_1, \ldots, g_N)$ with N-independent elements. ε_i are statistically independent entries with a zero mean and a unit variance

$$\langle \varepsilon_k \rangle = 0, \quad \langle \varepsilon_k^2 \rangle = 1, \tag{A2}$$

while j^0 scales with the matrix size N as $j^0 \propto N^{-\gamma_0/2}$. Note that the translation-invariant case of $g = (1, \ldots, 1)$ corresponds to the finite mean j^0 of the hopping elements (plus additional unimportant shift of energy).

As type-1 Hamiltonian [16,17] H_0 provides an exact eigenproblem solution [16]

$$\psi_{E_n}(k) = C_n \frac{g_k^*}{E_n - \varepsilon_k} , \tag{A3}$$

with the (possibly N-dependent) normalization constant $C_n = j^0 \sum_m g_m \psi_{E_n}(m)$,

$$|C_n|^{-2} = \sum_k \frac{|g_k|^2}{(E_n - \varepsilon_k)^2} , \tag{A4}$$

and the secular equation for the spectrum $E = E_n$

$$\sum_m \frac{|g_m|^2}{E - \varepsilon_m} = \frac{1}{j^0} \sim N^{\gamma_0/2} , \tag{A5}$$

giving all eigenvalues (except the highest one $E_N > \varepsilon_N$) lying between adjacent bare levels

$$\varepsilon_m < E_m < \varepsilon_{m+1} . \tag{A6}$$

Here we assumed ε_m to be ordered in ascending order $\varepsilon_m < \varepsilon_{m+1}$, $m = \overline{1, N-1}$. Note that this model includes the limiting case $a = 0$ of long-range deterministic hoppings considered in Ref. [18] both for positive ($g_m = 1$) and staggering ($g_m = (-1)^m$) hopping elements.

2. Spectral statistics

To find the spectrum E_n, one should consider the secular equation in more details. Let's assume that all g_k are of the same order $g_k \simeq g \sim N^0$ and consider the variation of E_n from its bare value ε_n as

$$\Gamma_n = E_n - \varepsilon_n, \quad 0 \leqslant \Gamma_n < \varepsilon_{n+1} - \varepsilon_n . \tag{A7}$$

Separating positive and negative summands of the sum (A5) for $E = E_n$, we obtain

$$\begin{aligned} \frac{1}{j^0} &= \frac{|g_n|^2}{\Gamma_n} + \sum_{k>0} \left[\frac{|g_{n-k}|^2}{\varepsilon_n - \varepsilon_{n-k} + \Gamma_n} - \frac{|g_{n+k}|^2}{\varepsilon_{n+k} - \varepsilon_n - \Gamma_n} \right] \\ &\simeq \frac{|g|^2}{\Gamma_n} + \sum_{k>0} \left[\frac{|g|^2}{\varepsilon_n - \varepsilon_{n-k} + \Gamma_n} - \frac{|g|^2}{\varepsilon_{n+k} - \varepsilon_n - \Gamma_n} \right] . \end{aligned} \tag{A8}$$

Now we have to estimate a typical value of the sum taking into account the inequality (A7). To do so we consider two limiting cases.

(i) In the limit of a completely rigid spectrum $\varepsilon_n = n\delta$, with the mean level spacing $\delta \sim 1/[\rho(0)N]$ and the density of states at the Fermi level $\rho(0)$, the sum (A8) can be taken explicitly

$$\frac{1}{|g|^2 j^0} = \frac{\pi}{\delta \tan(\pi \Gamma_n/\delta)} \tag{A9}$$

giving

$$\Gamma_n = \frac{\delta}{\pi} \arctan(\pi |g|^2 j^0/\delta) \sim N^{-\gamma_{\mathrm{YS}}/2} , \tag{A10}$$

where

$$\gamma_{\mathrm{YS}} = \max(\gamma_0, 2) . \tag{A11}$$

Analogously the normalization constant governed by (A4) takes the form

$$\begin{aligned} \frac{1}{|g|^2 |C_n|^2} &\simeq \sum_k \frac{1}{(\Gamma_n + \varepsilon_n - \varepsilon_k)^2} \\ &\simeq \frac{1}{\Gamma_n^2} + \frac{\pi^2}{\delta^2 \sin^2(\pi \Gamma_n/\delta)} \simeq \frac{1}{\Gamma_n^2} . \end{aligned} \tag{A12}$$

In the latter equality we neglect prefactors, focus only on the N scaling and take into account that $\Gamma_n \lesssim \delta$.

(ii) In the opposite limit of uncorrelated eigenstates, one can calculate (A8) as follows:

$$\frac{1}{|g|^2 j^0} = \frac{1}{\Gamma_n} + N\int_{|\omega|>\delta} \frac{\rho(\varepsilon_n-\omega)d\omega}{\omega+\Gamma_n} \simeq \frac{1}{\Gamma_n} + N\rho(0)\int_\delta^\infty d\omega\left[\frac{1}{\omega+\Gamma_n} - \frac{1}{\omega-\Gamma_n}\right] = \frac{1}{\Gamma_n} + \frac{1}{\delta}\ln\left(\frac{\delta-\Gamma_n}{\delta+\Gamma_n}\right), \tag{A13}$$

where we take into account (A7) in the lower limits of integration. Here the density of states is

$$\rho(\varepsilon) = \frac{1}{N}\sum_k \langle\delta(\varepsilon-\varepsilon_k)\rangle\,. \tag{A14}$$

Again considering only N scaling of Γ_n in (A13), one can obtain

$$\Gamma_n \sim N^{-\gamma_{\rm YS}/2}\,. \tag{A15}$$

Analogously the normalization constant governed by (A4) takes the form of (A12)

$$\frac{1}{|g|^2|C_n|^2}\frac{1}{\Gamma_n^2} + N\rho(0)\int_\delta^\infty d\omega\left[\frac{1}{(\omega+\Gamma_n)^2} - \frac{1}{(\omega-\Gamma_n)^2}\right] = \frac{1}{\Gamma_n^2} + \frac{1}{\delta}\left(\frac{1}{\delta+\Gamma_n} - \frac{1}{\delta-\Gamma_n}\right) \simeq \frac{1}{\Gamma_n^2}\,. \tag{A16}$$

As the scaling [(A10) and (A15)] of the energy deviation Γ_n (A7) and of the normalization constant C_n [(A12) and (A16)] are the same in both limiting cases, we conclude that these parameters weakly depends on the statistics of bare levels ε_n.

3. Eigenstate statistics

Using the results (A3) and (A12), one can calculate the spectrum of fractal dimensions $f(\alpha)$ for the wave-function intensity

$$|\psi_{E_n}(k)|^2 = \frac{|C_n|^2|g|^2}{(E_n-\varepsilon_k)^2} \simeq \frac{1}{[(\varepsilon_n-\varepsilon_k)N^{\gamma_{\rm YS}/2}-1]^2} \equiv N^{-\alpha}\,. \tag{A17}$$

Indeed, as the probability of $\varepsilon_n-\varepsilon_k \sim N^{-p/2}$ for $p>0$ is

$$dP(\varepsilon_n-\varepsilon_k \sim N^{-p/2}) \sim P(p)dp \sim N^{-p/2}dp\,, \tag{A18}$$

one can easily find

$$\alpha = \begin{cases} \gamma_{\rm YS}-p, & p<\gamma_{\rm YS} \\ 0, & p>\gamma_{\rm YS} \end{cases} \tag{A19}$$

and

$$N^{f(\alpha)-1} = dP(p(\alpha)) \sim N^{-p(\alpha)/2} = N^{(\alpha-\gamma_{\rm YS})/2} \tag{A20}$$

for $p=\gamma_{\rm YS}-\alpha>0$, giving the spectrum of fractal dimensions of the form of [26]

$$f(\alpha) = 1 + \frac{\alpha-\gamma_{\rm YS}}{2}\,, \quad 0<\alpha<\gamma_{\rm YS}\,, \tag{A21}$$

with $\gamma_{\rm YS}$ given by (A11).

As a result, unlike the Rosenzweig-Porter model, the YS model (A1) shows only localized and critical wave functions of *all* eigenstates, except the only top energy state at $\gamma_0<2$ [17]. At $\gamma_0>2$, the wave-function statistics (A21) coincides with the one of the RP, with $\gamma_{\rm YS}=\gamma_0$, while at all $\gamma_0<2$ instead of the delocalized phases YS model shows the critical localization with $\gamma_{\rm YS}=2$.

APPENDIX B: MATRIX INVERSION TRICK

In this Appendix, we first give general estimate of the optimal parameter β, $E_0 \sim N^\beta$ and then apply the matrix inversion trick [19] to the PLRBM model with partial correlations (3)

1. Optimization over E_0 in the matrix inversion trick

Let's focus for simplicity on the case of $E \sim W \sim N^0$. The effective hopping matrix $J_{m-n} = M_{m-n}(E+E_0-\varepsilon_n)/M_0$ in Eq. (20)

$$[(1+\hat{j}^0/E_0)^{-1}(E-\hat{\varepsilon}+E_0)-E_0]|\psi_E\rangle = 0 \tag{B1}$$

can be estimated as follows:

$$\hat{J} = \sum_p |p\rangle\langle p|\frac{E+E_0}{M_0(E_0+j_p^0)} \equiv \sum_p J_p|p\rangle\langle p|. \tag{B2}$$

Here we neglected the term ε_n for simplicity as $E\sim\varepsilon_n\sim N^0$ and divided Eq. (20) by

$$M_0 = \frac{1}{N}\sum_p \frac{1}{E_0+j_p^0} \simeq \frac{1}{E_0+j_{p,\min}^0} \tag{B3}$$

in order to have diagonal disorder in the standard form of ε_n. Here $j_{p,\min}^0$ is the typical hopping energy level and E_0 is taken to be in the gap of the hopping spectrum or beyond it (see Fig. 5).

Each term in the sum (B2) can be minimized over E_0 giving

$$E_0 \sim \min\left(|j_{p,\min}^0|, |E|\right), \quad J_p \simeq \frac{E|j_{p,\min}^0|}{j_{p,\min}^0+j_p^0}\,. \tag{B4}$$

However, one should take into account that E_0 has to be beyond the spectrum $|E_0| \gtrsim |j_{p,\min}^0|$, leading to the final result

$$E_0 \simeq j_{p,\min}^0, \quad J_p \simeq \frac{(E+j_{p,\min}^0)j_{p,\min}^0}{j_{p,\min}^0+j_p^0}\,. \tag{B5}$$

In the case of BM or YS deterministic hopping $\hat{j}^0$, the typical energy level $j_{p,\min}^0 \sim N^0$, thus, the optimal $E_0 \sim N^0$ and this confirms the statement given in the main text.

2. Matrix inversion for PLRBM model with partial correlations

We start with the model (1), (6) with $\tilde{j}_{mn} = |m-n|^{-\tilde{a}}$, $j_{mn}^0 = |m-n|^{-a_0}$ and compute matrix elements $\tilde{j}_{mn}^0 + r_{mn}$ of the effective Hamiltonian (22)

$$\hat{\tilde{j}}^0 + \hat{\tilde{j}} + \hat{r} = (1+\hat{j}^0/E_0)^{-1}(E-\hat{\varepsilon}+E_0+\hat{\tilde{j}})\,. \tag{B6}$$

The first terms in the brackets of right-hand side $(1+\hat{j}^0/E_0)^{-1}(E-\hat{\varepsilon}+E_0)$ scales as $|n|^{-(2-a)}$ at $a<1$ and correspond to $(1-\alpha)\hat{\tilde{j}}^0$ with a certain constant α of order of one. The calculation of it is given in Ref. [19]. Further we consider the rest part

$$\alpha\hat{\tilde{j}}^0 + \hat{\tilde{j}} + \hat{r} \equiv (1+\hat{j}^0/E_0)^{-1}\hat{\tilde{j}}\,. \tag{B7}$$

In order to simplify the calculations, we provide the upper bound of this term by replacing the oscillating amplitudes h_{mn} of $\tilde{j}_{mn} = h_{mn}/|m-n|^{\tilde{a}}$ by their maximal absolute value $h_{mn} = 1$. Within this approximation the result can be easily derived in the momentum space, since both matrices are diagonal in that basis. For purposes of clarity, we reproduce main steps of similar calculations presented in Ref. [19] specifically for the case of our interest.

We start by writing down the Fourier-transformed hopping amplitude j^0 (in case of $\tilde{j}$ one needs to replace a_0 by $\tilde{a}$) in different asymptotic regimes

$$j_p^0/2 \simeq \zeta_{a_0} + A_{a_0}\left(\frac{N}{|p|}\right)^{1-a_0}, \quad \text{for } |p| \ll N\,, \tag{B8}$$

$$j_p^0/2 \simeq j_{\min}^0 + B_{a_0}\left(\frac{2q}{N}\right)^{2}, \quad \text{for } q = |N/2 - p| \ll N\,, \tag{B9}$$

where the corresponding constants are given for $a_0 > 0$ by

$$A_{a_0} = (2\pi)^{a_0-1}\Gamma_{1-a_0}\sin\frac{\pi a_0}{2}\,, \tag{B10}$$

for $a_0 \neq 2m+1, m \in \mathbb{N}$ and

$$j_{\min}^0 = 2(2^{1-a_0}-1)\zeta_{a_0} < 0\,, \tag{B11}$$

$$B_{a_0} = 8\pi^2(1-2^{3-a_0})\zeta_{a_0-2} \simeq 2\pi^2 a_0 > 0\,. \tag{B12}$$

Here, ζ_{a_0} is the Riemann zeta function.

The next step is to estimate the long-range asymptotic behavior of the effective Hamiltonian $(1-\alpha)\hat{\tilde{j}}^0 + \hat{\tilde{j}} + \hat{r}$ given by

$$(1-\alpha)\tilde{j}_n^0 + \tilde{j}_n + r_n = C_0(a_0,\tilde{a}) + \frac{2}{N}\mathrm{Re}\sum_{p=1}^{N/2}\frac{\tilde{j}_p\, e^{2\pi i p n/N}}{E_0 + j_p^0} \tag{B13}$$

with the zero-momentum contribution

$$C_0(a_0,\tilde{a}) = \frac{\zeta_{\tilde{a}} + N^{1-\tilde{a}}/(1-\tilde{a})}{N(E_0/2+\zeta_{a_0}) + N^{2-a_0}/(1-a_0)}\,. \tag{B14}$$

The last term in (B13) can be split into three parts corresponding to different regimes of $\tilde{j}_p$ and j_p^0. However, not all of the resulting terms are equally important in the limit $1 \ll n \ll N$. One can easily show that summation only over sufficiently small momenta $|p| < \alpha N$ (where $0 < \alpha < 1/2$) contributes to the long-range behavior of matrix elements. The rest of the summation results in the gives small contribution to the residue term r_n and is unimportant. Thus we focus only on the following sum:

$$S(a_0,\tilde{a}) = \frac{2\zeta_{\tilde{a}}}{N}\mathrm{Re}\sum_{p=1}^{N\alpha_1}\frac{e^{2\pi i p n/N}}{E_0/2+\zeta_{a_0}+A_{a_0}(p/N)^{a_0-1}} + \frac{2A_{\tilde{a}}}{N}\mathrm{Re}\sum_{p=1}^{N\alpha_1}\frac{(p/N)^{\tilde{a}-1}e^{2\pi i p n/N}}{E_0/2+\zeta_{a_0}+A_{a_0}(p/N)^{a_0-1}}\,. \tag{B15}$$

In the case of our main interest ($a_0 < 1$) an additional momentum scale $p_c = N[E_0/2A_{a_0} + \zeta_{a_0}/A_{a_0}]^{-1/(1-a_0)} \leqslant N$ emerges, and for $p < p_c$ the denominator is represented by the power-law contribution. Contrary, for $p > p_c$, a constant term is dominant and we get

$$S(N\alpha, a_0 < 1, \tilde{a}) \approx \frac{\zeta_{\tilde{a}}A_{a_0-1}}{\pi A_{a_0}}\frac{1}{|n|^{2-a_0}} + \frac{A_{\tilde{a}}A_{1-\tilde{a}}}{\pi\left(E_0/2+\zeta_{a_0}\right)}\frac{1}{|n|^{\tilde{a}}} + \frac{A_{\tilde{a}}A_{a_0-\tilde{a}}}{\pi A_{a_0}}\frac{1}{|n|^{1-a_0+\tilde{a}}}\,, \tag{B16}$$

which for $a_0 < 1$ leads to the effective parameter governing the long-range tails of typical wave functions:

$$a_{\text{eff}} = \min(\tilde{a}, 2-a_0) \tag{B17}$$

in full agreement with the result (17b) mentioned in the main text. The last term in (B16) contribute to the residual term as it is small compared to the second term $\sim|n|^{-\tilde{a}}$ in the considered interval $a_0 < 1$.

APPENDIX C: SELF-CONSISTENT METHOD

In this Appendix, we use the formulation of the eigenproblem in terms of exact Eqs. (26)–(31) in order to derive expressions for scaling (35) of the broadening factor Γ_n in the average wave-function intensity (28).

In the first part we restrict our consideration to the first and second moments of the parameters a_n, P_{kn}, calculate sums S_1 (34) and S_2 (see below) in two limiting cases of (i) the completely rigid spectrum $\varepsilon_n - \varepsilon_m = (n-m)\delta$ and (ii) the Poisson statistics of ε_n, derive the mean expressions (32) for the RP model with partial correlations and the effective expression (35) for the broadening parameter Γ_n depending solely on S_1. Next, we explicitly calculate N scaling (35) of Γ_n.

1. Decoupling of correlations

In order to solve Eqs. (31), we assume that P_{kn} and a_n are uncorrelated from each other and from h_{lm} and calculate the mean and the variance for each of them averaging over off-diagonal matrix elements $h_{kn} = h_{nk}$ assumed to be real and taking into account $\langle h_{lm}\rangle = 0$, $\langle h_{lm}^2\rangle = 1$. As a result for $k \neq n$,

$$\langle P_{kn}\rangle = \sum_{l\neq n}\tilde{j}\langle h_{kl}\rangle\frac{\langle a_n + P_{\ln} + \tilde{j}h_{\ln}\rangle}{\omega_{nl}+\Gamma_n} = 0\,,$$

$$\langle P_{nn}\rangle = \sum_{l\neq n}\frac{\tilde{j}\langle h_{nl}\rangle\langle a_n + P_{\ln}\rangle + \tilde{j}^2\langle h_{\ln}^2\rangle}{\omega_{nl}+\Gamma_n} \equiv \tilde{j}^2 S_1\,,$$

$$\frac{\langle a_n\rangle}{j^0} = 1 + \sum_{l\neq n}\frac{\langle a_n\rangle + \tilde{j}\langle h_{\ln}\rangle + \langle P_{\ln}\rangle}{\omega_{nl}+\Gamma_n} \equiv 1 + \langle a_n\rangle S_1\,,$$

$$\left\langle P_{kn}^2\right\rangle = \tilde{j}^2\sum_{l,l'\neq n}\langle h_{kl}h_{kl'}\rangle\frac{\langle(a_n + P_{\ln} + \tilde{j}h_{\ln})(a_n + P_{l'n} + \tilde{j}h_{l'n})\rangle}{(\omega_{nl}+\Gamma_n)(\omega_{nl'}+\Gamma_n)}$$

$$= \tilde{j}^2 \sum_{l\neq n} \frac{\langle a_n^2\rangle + \langle P_{\rm ln}^2\rangle + \tilde{j}^2\langle h_{\rm ln}^2\rangle}{(\omega_{nl}+\Gamma_n)^2}$$
$$\equiv \tilde{j}^2 S_2\big(\langle a_n\rangle^2 + \sigma_a^2 + \langle P_{\rm ln}^2\rangle + \tilde{j}^2\big)\,,$$

$$\sigma_P^2 = \langle P_{nn}^2\rangle - \langle P_{nn}\rangle^2$$
$$= \tilde{j}^2 \sum_{l,l'\neq n} \left\langle h_{nl}h_{nl'} \frac{(a_n + P_{\rm ln} + \tilde{j}h_{\rm ln})(a_n + P_{l'n} + \tilde{j}h_{l'n})}{(\omega_{nl}+\Gamma_n)(\omega_{nl'}+\Gamma_n)} \right\rangle$$
$$-\tilde{j}^4 S_1^2$$
$$= \tilde{j}^2 \sum_{l\neq n} \frac{\langle a_n^2\rangle + \langle P_{\rm ln}^2\rangle + 3\tilde{j}^2}{(\omega_{nl}+\Gamma_n)^2} + \sum_{l\neq l'\neq n} \frac{\tilde{j}^4}{(\omega_{nl}+\Gamma_n)(\omega_{nl'}+\Gamma_n)}$$
$$-\tilde{j}^4 S_1^2$$
$$= \tilde{j}^2 S_2\big(\langle a_n\rangle^2 + \sigma_a^2 + \langle P_{\rm ln}^2\rangle + 2\tilde{j}^2\big)\,,$$

$$\frac{\sigma_a}{(j^0)^2} = \frac{\langle a_n^2\rangle - \langle a_n\rangle^2}{(j^0)^2}$$
$$= \sum_{l,l'\neq n} \left\langle \frac{(a_n + P_{\rm ln} + \tilde{j}h_{\rm ln})(a_n + P_{l'n} + \tilde{j}h_{l'n})}{(\omega_{nl}+\Gamma_n)(\omega_{nl'}+\Gamma_n)} \right\rangle$$
$$- \langle a_n - j^0\rangle^2$$
$$= \sum_{l\neq n} \frac{\langle P_{\rm ln}^2\rangle + \tilde{j}^2}{(\omega_{nl}+\Gamma_n)^2} + \sum_{l,l'\neq n} \frac{\langle a_n^2\rangle - \langle a_n\rangle^2}{(\omega_{nl}+\Gamma_n)(\omega_{nl'}+\Gamma_n)}$$
$$= \big(\langle P_{\rm ln}^2\rangle + \tilde{j}^2\big)S_2 + \sigma_a^2 S_1^2\,.$$

Here and further we use the notation $\omega_{nl} = \varepsilon_n - \varepsilon_l$ for brevity.

This gives the following self-consistency equations:

$$\langle P_{kn}\rangle = \tilde{j}^2 S_1 \delta_{kn}\,, \tag{C1a}$$
$$\langle a_n\rangle = \frac{1}{(j^0)^{-1} - S_1} \sim \min\left(j_0, S_1^{-1}\right), \tag{C1b}$$
$$\langle P_{kn}^2\rangle = \frac{\langle a_n\rangle^2 + \sigma_a^2 + \tilde{j}^2}{1 - (\tilde{j}^2 S_2)^{-1}}$$
$$\sim \big(\langle a_n\rangle^2 + \sigma_a^2 + \tilde{j}^2\big)\min(1, \tilde{j}^2 S_2)\,, \tag{C1c}$$
$$\sigma_P^2 = \langle P_{kn}^2\rangle + \tilde{j}^4 S_2\,, \tag{C1d}$$
$$\sigma_a^2 = \frac{\big(\langle P_{\rm ln}^2\rangle + \tilde{j}^2\big)S_2}{(j^0)^{-2} - S_1^2}$$
$$\sim \frac{S_2}{S_1^2}\big(\langle P_{\rm ln}^2\rangle + \tilde{j}^2\big)\min(1, (j^0 S_1)^2)\,, \tag{C1e}$$

with the sums

$$S_1 = \sum_{l\neq n} \frac{1}{\omega_{nl}+\Gamma_n},\ S_2 = \sum_{l\neq n} \frac{1}{(\omega_{nl}+\Gamma_n)^2}\,.$$

While averaging the denominators $\omega_{nl} + \Gamma_n$ we estimate only N scaling of the broadening parameter as follows:

$$\Gamma_n \sim \tilde{j} + \langle a_n\rangle + \langle P_{nn}\rangle + \sigma_a + \sigma_P \tag{C2}$$

and we consider the typical energy position ε_n to lie a bit asymmetrically in the middle of the spectrum, thus the summation would be in the limits $W_1 < \omega_{nl} < W_2$, with $|W_1 - W_2| \sim O(1)$ and $W_1 + W_2 = W$.

To estimate a typical value of the sums (33), we consider two limiting cases.

(i) In the limit of the completely rigid spectrum $\varepsilon_n = n\delta$, with the mean bare level spacing $\delta \sim 1/[\rho(0)N] \sim W/N$ and the density of states at the Fermi level $\rho(0)$, the sums can be taken explicitly

$$S_1 = \begin{cases} \frac{\ln(W_2/W_1)}{\delta} + \frac{\pi}{\delta\tan(\pi\Gamma_n/\delta)} - \frac{1}{\Gamma_n}, & \Gamma_n \ll W \\ \frac{N}{\Gamma_n}, & \Gamma_n \gg W \end{cases};$$

$$S_2 = \begin{cases} \frac{\pi^2}{\delta^2} + \frac{\pi^2}{\delta^2\sin^2(\pi\Gamma_n/\delta)} - \frac{1}{\Gamma_n^2}, & \Gamma_n \ll W \\ \frac{N}{\Gamma_n^2}, & \Gamma_n \gg W \end{cases}$$

and provide the following asymptotics:

$$S_1 \sim \begin{cases} \frac{1}{\delta}, & \Gamma_n \ll W \\ \frac{N}{\Gamma_n}, & \Gamma_n \gg W \end{cases}; \tag{C3a}$$
$$S_2 \sim \begin{cases} \frac{1}{\delta^2}, & \Gamma_n \ll W \\ \frac{N}{\Gamma_n^2}, & \Gamma_n \gg W \end{cases}. \tag{C3b}$$

(ii) In the opposite limit of uncorrelated eigenstates, one can calculate (33) as follows:

$$S_1 = \frac{N}{2}\left[\int_{-W_1}^{-\delta} \frac{\rho(\varepsilon_n - \omega)d\omega}{\omega + \Gamma_n} + \int_{\delta}^{W_2} \frac{\rho(\varepsilon_n - \omega)d\omega}{\omega + \Gamma_n}\right]$$
$$\simeq \frac{N\rho(0)}{2}\left[\int_{\delta}^{W_1} \frac{d\omega}{\omega + \Gamma_n} - \int_{\delta}^{W_2} \frac{d\omega}{\omega - \Gamma_n}\right]$$
$$= \frac{1}{2\delta}\left[\ln\left|\frac{W_1 + \Gamma_n}{W_2 - \Gamma_n}\right| - \ln\left|\frac{\delta - \Gamma_n}{\delta + \Gamma_n}\right|\right],$$

$$S_2 = \frac{N}{2}\left[\int_{-W_1}^{-\delta} \frac{\rho(\varepsilon_n - \omega)d\omega}{(\omega + \Gamma_n)^2} + \int_{\delta}^{W_2} \frac{\rho(\varepsilon_n - \omega)d\omega}{(\omega + \Gamma_n)^2}\right]$$
$$\simeq \frac{N\rho(0)}{2}\left[\int_{\delta}^{W_1} \frac{d\omega}{(\omega + \Gamma_n)^2} + \int_{\delta}^{W_2} \frac{d\omega}{(\omega - \Gamma_n)^2}\right]$$
$$= \frac{N}{(\Gamma_n - W_1)(\Gamma_n - W_2)} - \frac{1}{\Gamma_n^2 - \delta^2}\,.$$

Unlike YS model (A13) here the broadening parameter can be both smaller and larger than bare mean level spacing δ, thus, during the calculation we just take into account the fact that $E_n - \varepsilon_k = \omega + \Gamma_n$ is off-resonant. Here the density of states is $\rho(\varepsilon) = \sum_k \langle\delta(\varepsilon - \varepsilon_k)\rangle/N$.

In this case, asymptotics read as follows:

$$S_1 \sim \begin{cases} \frac{1}{\delta}, & \Gamma_n \ll W \\ \frac{N}{\Gamma_n}, & \Gamma_n \gg W \end{cases}; \tag{C4a}$$
$$S_2 \sim \begin{cases} \frac{1}{\delta^2}, & \Gamma_n \ll \delta \\ \frac{1}{\Gamma_n^2} + \frac{1}{\delta}, & \delta \ll \Gamma_n \ll W \\ \frac{N}{\Gamma_n^2}, & \Gamma_n \gg W \end{cases}. \tag{C4b}$$

Note that the expressions for sum S_1 are the same in both cases, while S_2 are different only in the nonergodic extended phase. Let's show that this difference do not affect the result (35) for the broadening parameter Γ_n. In order to prove it we consider the expression (C2) in more details substituting the expressions (C1) one by one.

First, let's substitute σ_P

$$\Gamma_n \sim \tilde{j} + \langle a_n \rangle + \langle P_{nn} \rangle + \sigma_a + \tilde{j}^2\sqrt{S_2} + (\langle a_n \rangle + \sigma_a + \tilde{j}) \min(1, \tilde{j}\sqrt{S_2}) .$$

As $\min(1, \tilde{j}\sqrt{S_2}) \leqslant 1$ one can neglect the whole last summand corresponding to $\sqrt{\langle P_{kn}^2 \rangle}$ which not larger than $\langle a_n \rangle + \sigma_a + \tilde{j}$. Next, we substitute σ_a

$$\Gamma_n \sim \tilde{j} + \langle a_n \rangle + \langle P_{nn} \rangle + \frac{\sqrt{S_2}}{S_1}\left(\sqrt{\langle P_{kn}^2 \rangle} + \tilde{j}\right) \min(1, j^0 S_1) + \tilde{j}^2\sqrt{S_2} .$$

As $S_1^2 \geqslant S_2$ in all phases of both limiting cases, one can neglect $\tilde{j}^2\sqrt{S_2}$ comparing to $\langle P_{nn} \rangle \sim \tilde{j}^2 S_1$ and the whole σ_a term comparing to $\langle a_n \rangle + \tilde{j}$ as $(\sqrt{S_2}/S_1)\min(1, j^0 S_1) \leqslant 1$. As a result we come to the expression (35)

$$\Gamma_n \sim \tilde{j} + \langle a_n \rangle + \langle P_{nn} \rangle \sim \tilde{j} + \min\left(j_0, S_1^{-1}\right) + \tilde{j}^2 S_1 , \quad \text{(C5)}$$

depending solely on S_1. This confirms the statement given in the main text and concludes this section.

2. Calculation of N scaling (35) of Γ_n

Using Eq. (C5) and expressions (C3) and (C4) for S_1, in this section we calculate the scaling (35) of Γ_n in all three phases:

(1) $\Gamma_n \gg W$. In this case, $S_1 = N/\Gamma_n$ and Eq. (C5) takes the form

$$\Gamma_n \sim N^{-\tilde{\gamma}/2} + \min\left(N^{-\gamma_0/2}, \frac{\Gamma_n}{N}\right) + \frac{N^{1-\tilde{\gamma}}}{\Gamma_n} . \quad \text{(C6)}$$

The second term does not play any role as it is less than $\Gamma_n/N \ll \Gamma_n$, while the third term dominates over the first one and gives $\Gamma_n \sim N^{(1-\tilde{\gamma})/2}$ and thus $\tilde{\gamma} < 1$.

(2) $\delta \ll \Gamma_n \ll W$. In this case, $S_1 = 1/\delta \sim N$ leading to

$$\Gamma_n \sim N^{-\tilde{\gamma}/2} + \min(N^{-\gamma_0/2}, \delta) + N^{1-\tilde{\gamma}} . \quad \text{(C7)}$$

As in the previous case, the second term does not play any role as it is less than $\delta \ll \Gamma_n$, while the third term dominates over the first one and gives $\Gamma_n \sim N^{1-\tilde{\gamma}}$ and thus $1 < \tilde{\gamma} < 2$.

(3) $\Gamma_n \ll \delta$. Here, $S_1 \sim 1/\delta$ leading to $\tilde{\gamma} > 2$ and

$$\Gamma_n \sim N^{-\tilde{\gamma}/2} + \min(N^{-\gamma_0/2}, \delta) + N^{1-\tilde{\gamma}} . \quad \text{(C8)}$$

In this case, the first term dominates over the third one and the concurrence of the first two terms gives the desired result $\Gamma_n \sim N^{-\tilde{\gamma}/2} + N^{-\gamma_{\rm YS}/2} \sim N^{-\gamma_{\rm eff}/2}$, with $\gamma_{\rm eff}$ given by (17a).

[1] D. M. Basko, I. L. Aleiner, and B. L. Altshuler, Metal-insulator transition in a weakly interacting many-electron system with localized single-particle states, Ann. Phys. **321**, 1126 (2006).

[2] I. V. Gornyi, A. D. Mirlin, and D. G. Polyakov, Interacting Electrons in Disordered Wires: Anderson Localization and Low-T Transport, Phys. Rev. Lett. **95**, 206603 (2005).

[3] P. W. Anderson, Absence of diffusion in certain random lattices, Phys. Rev. **109**, 1492 (1958).

[4] M. Serbyn, Z. Papić, and D. A. Abanin, Local Conservation Laws and the Structure of the Many-Body Localized States, Phys. Rev. Lett. **111**, 127201 (2013).

[5] D. A. Huse, R. Nandkishore, and V. Oganesyan, Phenomenology of certain many-body-localized systems, Phys. Rev. B **90**, 174202 (2014).

[6] C. J. Turner, A. A. Michailidis, D. A. Abanin, M. Serbyn, and Z. Papić, Weak ergodicity breaking from quantum many-body scars, Nat. Phys. **14**, 745 (2018).

[7] C. J. Turner, A. A. Michailidis, D. A. Abanin, M. Serbyn, and Z. Papić, Quantum scarred eigenstates in a rydberg atom chain: Entanglement, breakdown of thermalization, and stability to perturbations, Phys. Rev. B **98**, 155134 (2018).

[8] S. Choi, C. J. Turner, H. Pichler, W. W. Ho, A. A. Michailidis, Z. Papić, M. Serbyn, M. D. Lukin, and D. A. Abanin, Emergent SU (2) Dynamics and Perfect Quantum Many-Body Scars, Phys. Rev. Lett. **122**, 220603 (2019).

[9] V. Khemani, C. R. Laumann, and A. Chandran, Signatures of integrability in the dynamics of rydberg-blockaded chains, Phys. Rev. B **99**, 161101(R) (2019).

[10] P. Sala, T. Rakovszky, R. Verresen, M. Knap, and F. Pollmann, Ergodicity-breaking arising from hilbert space fragmentation in dipole-conserving hamiltonians, arXiv:1904.04266.

[11] S. Pai and M. Pretko, Manifestation of quantum many-body scars in fracton systems, arXiv:1903.06173.

[12] S. Pai, M. Pretko, and R. M. Nandkishore, Localization in Fractonic Random Circuits, Phys. Rev. X **9**, 021003 (2019).

[13] M. Brenes, M. Dalmonte, M. Heyl, and A. Scardicchio, Many-Body Localization Dynamics from Gauge Invariance, Phys. Rev. Lett. **120**, 030601 (2018).

[14] H. Bernien, S. Schwartz, A. Keesling, H. Levine, A. Omran, H. Pichler, S. Choi, A. S. Zibrov, M. Endres, M. Greiner, V. Vuletić, and M. D. Lukin, Probing many-body dynamics on a 51-atom quantum simulator, Nature (London) **551**, 579 (2017).

[15] A. L. Burin and L. A. Maksimov, Localization and delocalization of particles in disordered lattice with tunneling amplitude with r^{-3} decay, Pis'ma v Zh. Exp. Theor. Fiz. **50**, 304 (1989) [Sov. Phys. JETP Lett. **50**, 338 (1989)].

[16] H. K. Owusu, K. Wagh, and E. A. Yuzbashyan, The link between integrability, level crossings and exact solution in quantum models, J. Phys. A **42**, 035206 (2009).

[17] R. Modak, S. Mukerjee, E. A. Yuzbashyan, and B. S. Shastry, Integrals of motion for one-dimensional anderson localized systems, New J. Phys. **18**, 033010 (2016).

[18] X. Deng, V. E. Kravtsov, G. V. Shlyapnikov, and L. Santos, Duality in Power-Law Localization in Disordered One-Dimensional Systems, Phys. Rev. Lett. **120**, 110602 (2018).

[19] P. A. Nosov, I. M. Khaymovich, and V. E. Kravtsov, Correlation-induced localization, Phys. Rev. B **99**, 104203 (2019).

[20] Note that the complete correlations of *certain* (not all) hopping elements affect the level statistics and provokes emergent integrals of motion leading to the localization in a certain (not necessarily coordinate) basis [19].

[21] M. L. Mehta, *Random Matrices* (Elsevier, Amsterdam, 2004).

[22] A. D. Mirlin, Y. V. Fyodorov, F.-M. Dittes, J. Quezada, and T. H. Seligman, Transition from localized to extended eigenstates in the ensemble of power-law random banded matrices, Phys. Rev. E **54**, 3221 (1996).

[23] Here and further we consider the systems only with the uncorrelated diagonal disorder and focus on independent Gaussian distributed on-site energies ϵ_n with zero mean $\langle\epsilon_n\rangle$ and the variance $\langle\epsilon_n\rangle^2 = W^2$.

[24] The multifractality at the critical point $a = 1$ is out of the focus of this paper, thus, we do not consider the additional parameter b determining the strength of multifractality via the bandwidth of the nearly constant amplitude of fluctuating hopping at $|m - n| < b$ [22,50].

[25] Recently it has been shown [86] that the Wigner-Dyson-like full ergodic phase realizes only at $a < 1/2$, while in the range $1/2 < a < 1$ the wave-function statistics is only weakly ergodic and not of the Porter-Thomas form (see also Ref. [19]).

[26] V. E. Kravtsov, I. M. Khaymovich, E. Cuevas, and M. Amini, A random matrix model with localization and ergodic transitions, New J. Phys. **17**, 122002 (2015).

[27] N. Rosenzweig and C. E. Porter, "Repulsion of energy levels" in complex atomic spectra, Phys. Rev. **120**, 1698 (1960).

[28] A. Pandey, Brownian-motion model of discrete spectra, Chaos Solitons Fractals **5**, 1275 (1995).

[29] E. Brézin and S. Hikami, Correlations of nearby levels induced by a random potential, Nucl. Phys. B **479**, 697 (1996).

[30] T. Guhr, Transitions toward quantum chaos: With supersymmetry from poisson to gauss, Ann. Phys. **250**, 145 (1996).

[31] A. Altland, M. Janssen, and B. Shapiro, Perturbation theory for the rosenzweig-porter matrix model, Phys. Rev. E **56**, 1471 (1997).

[32] H. Kunz and B. Shapiro, Transition from poisson to gaussian unitary statistics: The two-point correlation function, Phys. Rev. E **58**, 400 (1998).

[33] P. Shukla, Alternative technique for complex spectra analysis, Phys. Rev. E **62**, 2098 (2000).

[34] P. Shukla, Level statistics of anderson model of disordered systems: Connection to brownian ensembles, J. Phys: Condens. Matter **17**, 1653 (2005).

[35] A. De Luca, A. Scardicchio, V. E. Kravtsov, and B. L. Altshuler, Support set of random wave-functions on the bethe lattice, arXiv:1401.0019.

[36] V. E. Kravtsov, B. L. Altshuler, and L. B. Ioffe, Non-ergodic delocalized phase in anderson model on bethe lattice and regular graph, Ann. Phys. **389**, 148 (2018).

[37] D. Facoetti, P. Vivo, and G. Biroli, From non-ergodic eigenvectors to local resolvent statistics and back: A random matrix perspective, Europhys. Lett. **115**, 47003 (2016).

[38] K. Truong and A. Ossipov, Eigenvectors under a generic perturbation: Non-perturbative results from the random matrix approach, Europhys. Lett. **116**, 37002 (2016).

[39] M. Amini, Spread of wave packets in disordered hierarchical lattices, Europhys. Lett. **117**, 30003 (2017).

[40] P. von Soosten and S. Warzel, The phase transition in the ultrametric ensemble and local stability of dyson brownian motion, Electron J. Probab. **23**, 1 (2018).

[41] P. von Soosten and S. Warzel, Non-ergodic delocalization in the rosenzweig–porter model, Lett. Math. Phys. **109**, 905 (2019).

[42] C. Monthus, Statistical properties of the green function in finite size for anderson localization models with multifractal eigenvectors, J. Phys. A **50**, 295101 (2017).

[43] E. Bogomolny and M. Sieber, Eigenfunction distribution for the rosenzweig-porter model, Phys. Rev. E **98**, 032139 (2018).

[44] G. de Tomasi, M. Amini, S. Bera, I. M. Khaymovich, and V. E. Kravtsov, Survival probability in generalized rosenzweig-porter random matrix ensemble, SciPost Phys. **6**, 014 (2019).

[45] The same behavior as in RP-ensemble has been observed in periodically driven systems [87], in quantum computations [88,89], and in Sachdev-Ye-Kitaev [90,91], $(SYK_4 + SYK_2)$ many-body model [92–94].

[46] G. L. Celardo, R. Kaiser, and F. Borgonovi, Shielding and localization in the presence of long-range hopping, Phys. Rev. B **94**, 144206 (2016).

[47] E. Abrahams, P. W. Anderson, D. C. Licciardello, and T. V. Ramakrishnan, Scaling Theory of Localization: Absence of Quantum Diffusion in two Dimensions, Phys. Rev. Lett. **42**, 673 (1979).

[48] Here we take the scalar C in fully correlated models to be constant, as its statistics does not play any role, and consider cross-correlations $\langle j_{mn} j_{m'n'}\rangle$ instead of cross-covariances $\langle j_{mn} j_{m'n'}\rangle - \langle j_{mn}\rangle\langle j_{m'n'}\rangle \neq 0$ without loss of generality.

[49] L. S. Levitov, Delocalization of Vibrational Modes Caused by Electric Dipole Interaction, Phys. Rev. Lett. **64**, 547 (1990).

[50] F. Evers and A. D. Mirlin, Anderson transitions, Rev. Mod. Phys. **80**, 1355 (2008).

[51] Y. Y. Atas, E. Bogomolny, O. Giraud, and G. Roux, Distribution of the Ratio of Consecutive Level Spacings in Random Matrix Ensembles, Phys. Rev. Lett. **110**, 084101 (2013).

[52] The multifractal phase usually shows finite residual level repulsion, but the spectrum is characterized by a finite level compressibility. However, there are some examples (e.g., RP ensemble) where the level statistics is of Wigner-Dyson (Poisson) form for small (large) energy differences [26,44].

[53] A. Ossipov, Anderson localization on a simplex, J. Phys. A **46**, 105001 (2013).

[54] A. Rodriguez, V. A. Malyshev, and F. Dominguez-Adame, Quantum diffusion and lack of universal one-parameter scaling in one-dimensional disordered lattices with long-range coupling, J. Phys. A **33**, L161 (2000).

[55] A. Rodriguez, V. A. Malyshev, G. Sierra, M. A. Martin-Delgado, J. Rodriguez-Laguna, and F. Dominguez-Adame, Anderson Transition in Low-Dimensional Disordered Systems Driven by Long-Range Nonrandom Hopping, Phys. Rev. Lett. **90**, 027404 (2003).

[56] D. B. Balagurov, V. A. Malyshev, and F. Dominiquez-Adame, Phase coherence in tight-binding models with nonrandom long-range hopping, Phys. Rev. B **69**, 104204 (2004).

[57] F. A. B. F. de Moura, A. V. Malyshev, M. L. Lyra, V. A. Malyshev, and F. Dominguez-Adame, Localization properties of a one-dimensional tight-binding model with nonrandom

long-range intersite interactions, Phys. Rev. B **71**, 174203 (2005).
[58] L. S. Levitov, Absence of localization of vibrational modes due to dipole-dipole interaction, Europhys. Lett. **9**, 83 (1989).
[59] N. F. Mott, The electrical properties of liquid mercury, Philos. Mag. **13**, 989 (1966).
[60] D. J. Luitz and Y. Bar Lev, Emergent locality in systems with power-law interactions, Phys. Rev. A **99**, 010105(R) (2019).
[61] A. O. Maksymov, A. L. Burin, and M. Heyl (unpublished).
[62] J. T. Cantin, T. Xu, and R. V. Krems, Effect of the anisotropy of long-range hopping on localization in three-dimensional lattices, Phys. Rev. B **98**, 014204 (2018).
[63] X. Deng, A. L. Burin, and I. M. Khaymovich (unpublished).
[64] For the general YS model, the latter should be modified by $\langle n|g_0\rangle = g_n/G$, with $G^2 = \sum_n |g_n|^2$.
[65] T. L. M. Lezama, S. Bera, and J. H. Bardarson, Apparent slow dynamics in the ergodic phase of a driven many-body localized system without extensive conserved quantities, Phys. Rev. B **99**, 161106(R) (2019).
[66] E. J. Torres-Herrera and L. F. Santos, Dynamics at the many-body localization transition, Phys. Rev. B **92**, 014208 (2015).
[67] M. Távora, E. J. Torres-Herrera, and L. F. Santos, Power-law decay exponents: A dynamical criterion for predicting thermalization, Phys. Rev. A **95**, 013604 (2017).
[68] E. J. Torres-Herrera, A. M. García-García, and L. F. Santos, Generic dynamical features of quenched interacting quantum systems: Survival probability, density imbalance, and out-of-time-ordered correlator, Phys. Rev. B **97**, 060303(R) (2018).
[69] L. F. Santos and E. J. Torres-Herrera, Nonequilibrium many-body quantum dynamics: From full random matrices to real systems, Thermodynamics Quantum Regime **195**, 457 (2018).
[70] S. Bera, G. De Tomasi, I. M. Khaymovich, and A. Scardicchio, Return probability for the anderson model on the random regular graph, Phys. Rev. B **98**, 134205 (2018).
[71] I. M. Khaymovich, M. Haque, and P. A. McClarty, Eigenstate Thermalization, Random Matrix Theory, and Behemoths, Phys. Rev. Lett. **122**, 070601 (2019).
[72] N. Y. Yao, C. R. Laumann, S. Gopalakrishnan, M. Knap, M. Müller, E. A. Demler, and M. D. Lukin, Many-Body Localization in Dipolar Systems, Phys. Rev. Lett. **113**, 243002 (2014).
[73] R. Singh, R. Moessner, and D. Roy, Effect of long-range hopping and interactions on entanglement dynamics and many-body localization, Phys. Rev. B **95**, 094205 (2017).
[74] T. Botzung, D. Vodola, P. Naldesi, M. Müller, E. Ercolessi, and G. Pupillo, Algebraic localization from power-law interactions in disordered quantum wires, arXiv:1810.09779.
[75] S. Roy and D. E. Logan, Self-consistent theory of many-body localisation in a quantum spin chain with long-range interactions, arXiv:1903.04851.
[76] S. Nag and A. Garg, Can many-body localization persist in the presence of long-range interactions or long-range hopping? Phys. Rev. B **99**, 224203 (2019).
[77] A. L. Burin and Y. Kagan, Low-energy collective excitations in glasses. new relaxation mechanism for ultralow temperatures, Zh. Eksp. Teor. Fiz. **106**, 633 (1994) [JETP **80**(4), 761 (1995)].
[78] A. L. Burin, Many-body delocalization in a strongly disordered system with long-range interactions: Finite-size scaling, Phys. Rev. B **91**, 094202 (2015).
[79] A. L. Burin, Localization in a random xy model with long-range interactions: Intermediate case between single-particle and many-body problems, Phys. Rev. B **92**, 104428 (2015).
[80] I. V. Gornyi, A. D. Mirlin, D. G. Polyakov, and A. L. Burin, Spectral diffusion and scaling of many-body delocalization transitions, Ann. Phys. **529**, 1600360 (2017).
[81] K. S. Tikhonov and A. D. Mirlin, Many-body localization transition with power-law interactions: Statistics of eigenstates, Phys. Rev. B **97**, 214205 (2018).
[82] G. De Tomasi, Algebraic many-body localization and its implications on information propagation, Phys. Rev. B **99**, 054204 (2019).
[83] A. Ossipov and V. E. Kravtsov, t duality in supersymmetric theory of disordered quantum systems, Phys. Rev. B **73**, 033105 (2006).
[84] O. Yevtushenko and V. E. Kravtsov, Virial expansion for almost diagonal random matrices, J. Phys. A **36**, 8265 (2003).
[85] O. Yevtushenko and A. Ossipov, A supersymmetry approach to almost diagonal random matrices, J. Phys. A **40**, 4691 (2007).
[86] E. Bogomolny and M. Sieber, Power-law random banded matrices and ultrametric matrices: Eigenvector distribution in the intermediate regime, Phys. Rev. E **98**, 042116 (2018).
[87] S. Roy, I. M. Khaymovich, A. Das, and R. Moessner, Multifractality without fine-tuning in a floquet quasiperiodic chain, SciPost Phys. **4**, 25 (2018).
[88] V. N Smelyanskiy, K. Kechedzhi, S. Boixo, S. V. Isakov, H. Neven, and B. L. Altshuler, Non-ergodic delocalized states for efficient population transfer within a narrow band of the energy landscape, arXiv:1802.09542.
[89] K. Kechedzhi, V. N. Smelyanskiy, J. R. McClean, V. S Denchev, M. Mohseni, S. V. Isakov, S. Boixo, B. L. Altshuler, and H. Neven, Efficient population transfer via non-ergodic extended states in quantum spin glass, arXiv:1807.04792.
[90] S. Sachdev and J. Ye, Gapless Spin-Fluid Ground State in a Random Quantum Heisenberg Magnet, Phys. Rev. Lett. **70**, 3339 (1993).
[91] A. Kitaev, A simple model of quantum holography, (2015), talks at KITP on April 7th and May 27th 2015.
[92] T. Micklitz, F. Monteiro, and A. Altland, Non-ergodic extended states in the syk model, arXiv:1901.02389.
[93] A. Kamenev and H. Wang, Many-body localization in a modified *syk* model, (2019), APS March Meeting 2019, abstract H06.00006.
[94] A. Kamenev, Many-body localization in a modified *syk* model, (2018), talk in the conference "Random Matrices, Integrability and Complex Systems", Yad Hashimona, Israel.